# An efficient optimal design methodology for nonlinear multibody dynamics systems with application to vehicle occupant restraint systems

Guang Dong, Zheng-Dong Ma*, Gregory Hulbert and Noboru Kikuchi
Mechanical Engineering Department
The University of Michigan
Ann Arbor, MI, 48109
Email: dongg@umich.edu
Email: mazd@umich.edu
Email: hulbert@umich.edu
Email: kikuchi@umich.edu
*Corresponding author

Sudhakar Arepally, Madan Vunnam, and James Sheng
U.S. Army TARDEC
Warren, MI, 48397
Email: sudhakar.arepally@us.army.mil
Email: madanmohan.vunnam@us.army.mil
Email: james.sheng@us.army.mil

Ken-An Lou
ArmorWorks, LLC
Chandler, Arizona, 85226
Email: klou@armorworks.com

**Abstract**: The need exists for robust and efficient optimal design methods for application to multibody systems, in which the components to be designed represent connections between large displacement, large rotation motions of the subsystems' bodies. A specific application is an occupant restraint systems, such as the Gunner Restraint System (GRS), in which both the vehicle and the gunner can undergo large relative and absolute motions under extreme driving or external threat conditions. In addition, the restraint/connection components can have amplitude-dependent, time-dependent, and timing-dependent behavior, such as an active belt retractor. Current optimization methodologies are ill-suited for this problem, suffering from infeasibility, lack of robustness, and/or high computationally expense. This paper presents an extension of topology

# Report Documentation Page

*Form Approved*
*OMB No. 0704-0188*



| | | |
|---|---|---|
| 1. REPORT DATE<br>**01 APR 2011** | 2. REPORT TYPE<br>**N/A** | 3. DATES COVERED<br>**-** |

| | |
|---|---|
| 4. TITLE AND SUBTITLE<br>**An Efficient optimal design methodology for nonlinear multibody dynamics systems with application to vehicle occupant restraint systems (PREPRINT)** | 5a. CONTRACT NUMBER<br>**W56HZV-04-2-0001** |
| | 5b. GRANT NUMBER |
| | 5c. PROGRAM ELEMENT NUMBER |
| 6. AUTHOR(S)<br>**Guang Dong; Zheng-Dong Ma; Gregory Hulbert; Noboru Kikuchi; Sudhakar Arepally; Karrie Hope; Madan Vunnam; James Sheng; Ken-An Lou; Hui Wang** | 5d. PROJECT NUMBER |
| | 5e. TASK NUMBER |
| | 5f. WORK UNIT NUMBER |
| 7. PERFORMING ORGANIZATION NAME(S) AND ADDRESS(ES)<br>**US Army RDECOM-TARDEC 6501 E 11 Mile Rd Warren, MI 48397-5000, USA University of Michigan Ann Arbor, MI 48109 USA ArmorWorks, LLC Chandler, Arizona, 85226 USA AM General, LLC Livonia, MI 48150, USA** | 8. PERFORMING ORGANIZATION REPORT NUMBER<br>**21662RC** |
| 9. SPONSORING/MONITORING AGENCY NAME(S) AND ADDRESS(ES)<br>**US Army RDECOM-TARDEC 6501 E 11 Mile Rd Warren, MI 48397-5000, USA** | 10. SPONSOR/MONITOR'S ACRONYM(S)<br>**TACOM/TARDEC/RDECOM** |
| | 11. SPONSOR/MONITOR'S REPORT NUMBER(S)<br>**21662RC** |

12. DISTRIBUTION/AVAILABILITY STATEMENT
**Approved for public release, distribution unlimited**

13. SUPPLEMENTARY NOTES
**Submitted for publication ia a special issure of Int'l Journal of Vehicle Design, The original document contains color images.**

14. ABSTRACT

15. SUBJECT TERMS

| 16. SECURITY CLASSIFICATION OF: | | | 17. LIMITATION OF ABSTRACT | 18. NUMBER OF PAGES | 19a. NAME OF RESPONSIBLE PERSON |
|---|---|---|---|---|---|
| a. REPORT<br>**unclassified** | b. ABSTRACT<br>**unclassified** | c. THIS PAGE<br>**unclassified** | **SAR** | **37** | |

**Standard Form 298 (Rev. 8-98)**
Prescribed by ANSI Std Z39-18

optimization techniques to consider multibody dynamics systems and to treat the much more open design space, which can include passive, active, and reactive structures/devices. The objective is to obtain an optimally combined structural and material system, considering the best use of passive, active and reactive members. This paper highlights: 1) dealing with design objectives that consider time-dependent, dynamic, large deformation responses; 2) general representative models for the multi-disciplinary (passive, active or reactive) components in a multibody dynamics simulation system; 3) designing an optimal system that can satisfy multiple requirements under various operating conditions; 4) an efficient sensitivity analysis method for the optimization problem of the restraint system; and 5) a general and advanced optimization algorithm that can solve the problems.

**Keywords**: topology optimization, multibody dynamics, sensitivity analysis, restraint system, vehicle safety, automotive vehicles, active devices**.**

## 1. Introduction

Motivating this research is the need to design vehicle occupant restraint systems for improved occupants' safety under various operating conditions and often hazardous environments. Using a Gunner Restraint System as an example, the occupant (gunner) sits or stands in the passenger compartment with their upper torso, arms, and head exposed outside the top of the vehicle. The restraint system should not only be able to prevent the occupant from being ejected from the vehicle but also be able to assist rapid entry into the vehicle during a rollover or other accidents to avoid injury or fatality. For this application, the restraint system should also help stabilize the gunner over rough terrain and in high speed maneuver conditions for them to complete their functional tasks.

The restraint system may involve a wide range of possible usage of passive, active and reactive devices which could be mounted at many possible physical locations (interacting points) between the vehicle and the occupant. These devices may include safety elements such as belts, airbags and retractors and may have to be activated in a specific sequence or timing to protect the occupant in the designed situations. For the purposes of this paper, a passive device is defined as a structure or device that responds to the excitation passively without an active action. An active device is defined as a structure or device that can actively respond to the excitation with an energy supply for the operation. A reactive structure is defined as a class of smart structure that can react to external excitations in a specially designed way using the energy pre-stored in the system or from the external excitation to counteract the hazardous loading or perform other desired tasks. (Chiyo et al., 2010, Dong et al., 2009; Ma et al., 2006a; 2007; 2008; 2010) The design of a restraint system must also consider minimizing the system weight, complexity, and cost, while maximizing reliability, durability, and occupant friendly-ability.

More generally, the design problem of interest involves multiple multibody dynamics systems and their interconnections, which need to be designed to constrain the relative motions/positions of the multibody dynamics systems for given objectives, such as those related to the safety issues. The multibody dynamics systems can include flexible bodies; however, in this paper, we limit developments to rigid multibody dynamics systems for the purpose of exposition. The application focus is on the safety system design problems related to automotive vehicles, including military vehicles, such as gunner restraint systems, blast-protective seating systems and other restraint systems, and commercial applications, such as passenger safety and protection systems in passenger cars for protection against crash or rollover. Other applications vehicle transportation systems, space vehicle landing systems, ground and sea vehicles mooring systems. For a transportation system, the design objective can be the relative movement of the vehicle with respect to the carrier vehicle (ground, sea or air) for a transportation task in a dynamic environment. The design space could include connecting chains, networked belts, or other constraint mechanisms. For the optimal mooring system, the design objective could be the vessel's lateral and longitudinal accelerations and yawing movements. The design space can be all the possible interactions between the vessel and the dock with the objective to find the optimal mooring system.

Practical solution of these design problems requires a robust and efficient optimal design method to quickly layout an optimal restraint system between the multiple multibody systems, in which the components to be designed can represent connections between large displacements, large rotation motions of the subsystems' bodies. In addition, the connection components can have amplitude-dependent, time-dependent, and timing-dependent behaviors, such as that with an active belt retractor. Current optimization methodologies are ill-suited for this problem, suffering from feasibility, robustness, and/or efficiency. A fundamental multidisciplinary structure design methodology for multibody dynamics systems is presented. This design methodology identifies optimally combined multidisciplinary structural components with specific geometric and connectivity configurations and also mechanical properties for the given (multiple) design objectives. One challenge in developing such a design methodology comes from the complexity of general multibody dynamics systems and the wide open design space that covers passive, active and reactive devices with nonlinear, time-dependent and timing-dependent design variables.

Topology optimization for optimal structural design methodology has received extensive attention since Bendsøe and Kikuchi (1988) as seen by its wide application to many structural optimization problems (Bendsøe, 1989; 1995; Bendsøe and Sigmund, 2003; Ma et al., 1995b; 1995c; Sigmund, 2001). There are two major approaches towards topology optimization: one is the continuum based approach, while the second is the discrete component based approach. In the continuum based approach, the material is continuously distributed within a design domain by considering a specific variable (physical or artificial) material model in the design domain. In this approach, the structure is consequently optimized by varying the design variables associated with the material model. In the discrete component based approach, for example, the ground structure approach developed by Zhou and Rozvany (1991), a structural optimization problem is transformed to a problem of seeking the optimal layout in a design space that considers all the possible connection members between the predefined nodal points and the optimization is achieved by removing unnecessary connection members and reinforcing necessary connection members in the design space in improving the design objective.

The standard topology optimization method has been extended to a multi-domain topology optimization (MTO) method (Ma et al., 2006b) to consider a topology optimization problem with multiple domains by allowing assignment of different amounts of the materials, as well as of different materials, to the different sub-domains of a structure. This technique can be used to deal with a number of important applications, such as structure-fixture simultaneous design problems, functionally gradient material design problems, and crush energy management design problems.

Various optimization algorithms have been developed for usage in topology optimization, such as the Optimality Criteria (OC) method by Berke and Khot (1987), Sequential Linear Programming (SLP), Convex Linearization (CONLIN) method by Fleury and Brainbant (1986), the Method of Moving Asymptotes (MMA) by Svanberg (1987), Diagonal Sequential Quadratic Programming (DSQP) by Fleury (1987), Modified Optimality Criteria (MOC) method by Ma, Kikuchi and Hagiwara (1992) and Generalized Sequential Approximate Optimization (GASO) by Ma and Kikuchi (1995a). The GASO algorithm extends the compatibility of previous optimization algorithms by allowing more advanced updating rules and offering more flexibility for a wide range of optimization problems. The enhancement in the GSAO results in improved convergence, higher computational efficiency and a more stabilized iterative process for large-scale optimization problems, including those dealing with dynamic response. This method is ideal for multi-domain topology optimization problems and was be utilized in the present effort.

Topology optimization problems usually involve in a large number of design variables; therefore, an efficient sensitivity analysis method is critical for obtaining solutions within practical time limits. Efficient sensitivity analysis methods have been developed previously for topology optimization related to static response, eigenvalue, and frequency response. For example, Zhou and Rozvany (1991), computed sensitivities are based on the static response of a linear elastic structural system. Sensitivity calculations for dynamical systems are, however, fundamentally different from those for a static or quasi-static system. Sensitivity calculation is even more challenging when dealing with multibody dynamics systems, which are governed by sets of differential-algebraic equations (DAEs. In both the dynamic and multibody dynamic response problems, the governing equations are time-dependent and so are their sensitivities. For structural dynamic problems, there are two widely used sensitivity analysis methods: the direct differentiation method and the adjoint variable method (Hsieh and Arora, 1984). To carry out sensitivity analysis by the direct differentiation method, the dynamic equations need to be solved as many times as the number of design variables (Kang, Park and Arora, 2006). Therefore, this method in general is infeasible for topology optimization problems dealing with a large number of design variables. Cao, et al. (2003) proposed an adjoint variable sensitivity analysis method for systems governed by DAEs of index up to two. In this approach, a new set of DAEs for the adjoint variables is solved for obtaining the sensitivities (Alexe and Sandu, 2009). For complex multibody dynamics system models, the difficulty of solving the additional adjoint equations is significant. Recently, for topology optimization of a flexible multibody dynamic system, Bruls et al. (2009) proposed a sensitivity analysis method based on the general-α method (Chung and Hulbert, 1993). This method considers the dynamic effect of the multibody dynamics system based on the generalized-α method; it however still requires solving the dynamic equations for each design variable. Kang, Choi and Park (2001) proposed using simplified quasi-static load cases equivalent to the complicated loading for multibody dynamics system. However, it can be difficult to find equivalent static loading, and the optimization results based on equivalent static loading might be not able to converge to same optimization results with actual loading condition. (Bruls et al., 2009)

This paper presents an extension of the topology optimization method for geometrically nonlinear, time-dependent and timing-dependent multibody dynamics systems with the consideration of nonlinear response and a general multidisciplinary system design problem with the various options from using passive, active and reactive structures and devices. Of particular emphasis are: 1) dealing with design objectives that consider time- and timing-dependent, dynamic, large deformation responses; 2) general representative models for the multi-disciplinary (passive, active or reactive) components in a multibody dynamics simulation system; 3) designing an optimal system that can satisfy multiple requirements under various operating conditions; 4) an efficient sensitivity analysis method for the optimization problem of the occupant restraint system design; and 5) a general and advanced optimization algorithm that can be used to solve the design problems.

## 2. Description of the design problem

As shown in Figure 1, consider two general multibody dynamics systems, MDS-1 and MDS-2, interconnected by a set of $N$ connection members. Each multibody dynamics system has a number of rigid bodies linked by joints, bushings, and/or other internal constraints. As suggested in Figure 1, MDS-1 may represent a human body, while MDS-2 may represent a vehicle system. There are $n_1$ rigid bodies in MDS-1, and $n_2$ rigid bodies in MDS-2. The set of connection members may represent a possible system that restrains the relative motions between the two multibody dynamics systems. Each member in the restraint system can be described as an interaction force between the two interacting points at the two multibody dynamics systems. The interaction force may have non-linear dependency on the relative movement (displacement, velocity, and/or acceleration) of the points and it can be time-dependent and/or timing-dependent. It can also be passive, active, or reactive depending on the application.

**Figure 1** General description of the design problem

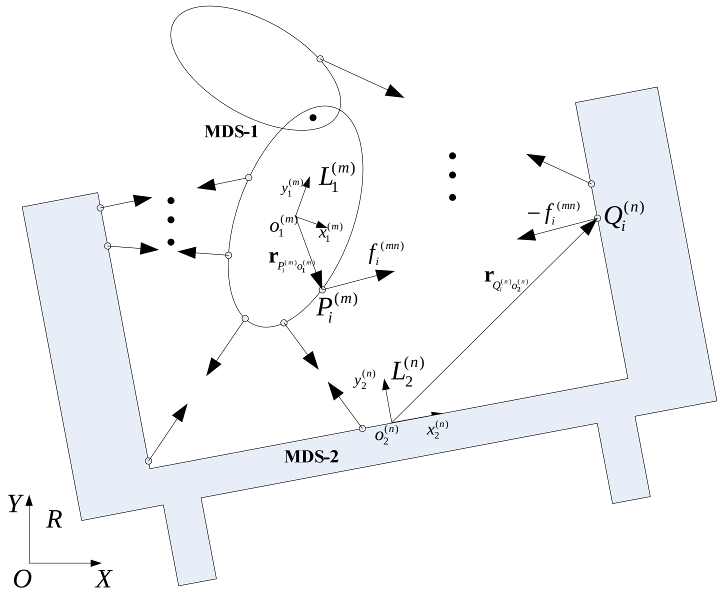


In general, the $i$th interaction force, which acts on $m$th body in MDS-1 and $n$th body in MDS-2, can be defined as

$$f_i = f_i(\Delta_i,\ \dot{\Delta}_i,\ t,\ t_i^{\mathbf{0}},\ \delta_i^{\mathbf{0}},\ \mathbf{p}_i) \tag{1}$$

Here $i$ denotes the $i$th interactive member, $\Delta_i$ denotes the relative distance change (deformation) between the two interacting points, in which $P_i^{(m)}$ is the interacting point of the $i$th interactive member of the $m$th body in the MDS-1, and $Q_i^{(n)}$ is the interacting point of the $i$th interactive member of the $n$th body in the MDS-2., $\dot{\Delta}_i$ denotes the speed (time directive of $\Delta_i$ ), $t_i^{\mathbf{0}}$ denotes the critical timing for activating the $i$th interactive member, $\delta_i^{\mathbf{0}}$ denotes an initial distance gap for the $i$th interactive member to become active, and $\mathbf{p}_i$ is a vector of other design parameters for the $i$th interactive member. For example, a simple form of $f_i$ is given by:

$$f_i = k_i\Delta_i + c_i\dot{\Delta}_i \tag{2}$$

A one way contact with a gap function can be defined as:

$$f_i = \begin{cases} \mathbf{0} & \Delta_i < \delta_i^{\mathbf{0}} \\ k_i\left(\Delta_i - \delta_i^{\mathbf{0}}\right) + c_i\dot{\Delta}_i & \Delta_i \geq \delta_i^{\mathbf{0}} \end{cases} \tag{3}$$

An active force function can be defined as

$$f_i = f_{\mathbf{0}i}\exp\left(-\lambda_i\left(t - t_{\mathbf{0}}\right)^2\right) \tag{4}$$

where $k_i$ and $c_i$ are stiffness and damping coefficient for the $i$th interactive member; $f_{\mathbf{0}i}$ and $\lambda_i$ are design parameters for the $i$th interactive member.

Since the $i$th interactive member connects the $m$th body in MDS-1 and the $n$th body in MDS-2, $f_i$ can also be denoted as $f_i^{(mn)}$; $\Delta_i$ can also be denoted as $\Delta_i^{(mn)}$. The direction of the interactive force $f_i^{(mn)}$ of the $i$th member is defined by $\mathbf{e}_i^{(mn)} = \frac{\mathbf{r}_{Q_i^{(n)}P_i^{(m)}}}{\left\|\mathbf{r}_{Q_i^{(n)}P_i^{(m)}}\right\|}$, where $\mathbf{r}_{Q_i^{(n)}P_i^{(m)}}$ denotes the line of action between $\overline{P_i^{(m)}Q_i^{(n)}}$, Therefore, the $i$th force vector acting on the MDS-1 is $\mathbf{f}_i^{\mathbf{1}} = f_i\mathbf{e}_i$, and the force vector of the same interaction member acting on the MDS-1 is $\mathbf{f}_i^{\mathbf{2}} = -f_i\mathbf{e}_i$, and we have $\mathbf{f}_i^{\mathbf{1}} + \mathbf{f}_i^{\mathbf{2}} = \mathbf{0}$. Let a global force vector $\mathbf{F}$ and global deformation vector $\mathbf{\Delta}$ be given as:

$$\mathbf{F} = \left\{f_1, \quad f_2, \quad \cdots \quad f_N\right\}^T \tag{5}$$

$$\mathbf{\Delta} = \left\{\Delta_1, \quad \Delta_2, \quad \cdots \quad \Delta_N\right\}^T \tag{6}$$

which represents the restraint system with a total of $N$ interaction forces.

Assume a global coordinate system $R: O - XYZ$, and local coordinate systems $L_{\mathbf{1}}^{(m)}: o_{\mathbf{1}}^{(m)} - x_{\mathbf{1}}^{(m)}y_{\mathbf{1}}^{(m)}z_{\mathbf{1}}^{(m)}$ with origin $o_{\mathbf{1}}^{(m)}$ attached to the mass center of $m$th body in MDS-1, $L_{\mathbf{2}}^{(n)}: o_{\mathbf{2}}^{(n)} - x_{\mathbf{2}}^{(n)}y_{\mathbf{2}}^{(n)}z_{\mathbf{2}}^{(n)}$ with origin $o_{\mathbf{2}}^{(n)}$ attached to the mass center of $n$th body in MDS-2. Assuming $\mathbf{q}_1 = [\mathbf{q}_1^{(1)T}, \mathbf{q}_1^{(2)T}, \ldots, \mathbf{q}_1^{(n_1)T}]^T$ is the generalized coordinates vector of MDS-1,

$\mathbf{q}_2 = [\mathbf{q}_2^{(1)T}, \mathbf{q}_2^{(2)T}, \ldots, \mathbf{q}_2^{(n_2)T}]^T$ is the generalized coordinates vector of MDS-2, the governing equation for MDS-1 can be written as:

$$\begin{cases} \mathbf{M}_1(\mathbf{q}_1)\ddot{\mathbf{q}}_1 - \mathbf{Q}_1 + (\mathbf{C}_1)_{\mathbf{q}_1}^T \boldsymbol{\lambda}_1 = \mathbf{F}_1^{Ext} + \mathbf{F}_1^q \\ \mathbf{C}_1(\mathbf{q}_1, \dot{\mathbf{q}}_1) = \mathbf{0} \end{cases} \tag{7}$$

where the first equation in (7) is the dynamic equilibrium equation, and the second equation is the constraint equation for MDS-1. $\mathbf{M}_1$ denotes the generalized mass matrix, $(\mathbf{C}_1)_{\mathbf{q}_1}$ denotes the Jacobian matrix of $\mathbf{C}_1$, $\boldsymbol{\lambda}_1$ denotes vector of Lagrangian multipliers. $\mathbf{Q}_1$ is the quadratic velocity term. $\mathbf{F}_1^{Ext}$ denotes the external force applied on MDS-1, $\mathbf{F}_1^q$ is the generalized force vector of MDS-1 due to the restraint system to be designed.

Similarly, the governing equation for MDS-2 can be written as:

$$\begin{cases} \mathbf{M}_2(\mathbf{q}_2)\ddot{\mathbf{q}}_2 - \mathbf{Q}_2 + (\mathbf{C}_2)_{\mathbf{q}_2}^T \boldsymbol{\lambda}_2 = \mathbf{F}_2^{Ext} + \mathbf{F}_2^q \\ \mathbf{C}_2(\mathbf{q}_2, \dot{\mathbf{q}}_2) = \mathbf{0} \end{cases} \tag{8}$$

in which $\mathbf{M}_2$ denotes the generalized mass matrix, $(\mathbf{C}_2)_{\mathbf{q}_2}$ denotes the Jacobian matrix of $\mathbf{C}_2$, $\boldsymbol{\lambda}_2$ denotes vector of Lagrangian multipliers. $\mathbf{Q}_2$ is the quadratic velocity term. $\mathbf{F}_2^{Ext}$ denotes the external force applied on MDS-2, $\mathbf{F}_2^q$ is the generalized force vector of MDS-2 due to the restraint system to be designed.

$\mathbf{F}_1^q$ and $\mathbf{F}_2^q$ are the generalized force vectors defined in the generalized coordinate systems for MDS-1 and MDS-2. In general, $\mathbf{F}_1^q$ and $\mathbf{F}_2^q$ can be written as

$$\mathbf{F}_1^q = \mathbf{B}_1^T\mathbf{F} \text{ and } \mathbf{F}_2^q = \mathbf{B}_2^T\mathbf{F} \tag{9}$$

or equivalently,

$$\begin{Bmatrix} \mathbf{F}_1^q \\ \mathbf{F}_2^q \end{Bmatrix} = \mathbf{B}^T \mathbf{F} \tag{10}$$

where $\mathbf{B} = \begin{bmatrix} \mathbf{B}_1 & \mathbf{B}_2 \end{bmatrix}$ is called *compatibility matrix*, which is a function of the generalized coordinates $\mathbf{q}_1$ and $\mathbf{q}_2$. $\mathbf{B}_1$ is the compatibility matrix for MDS-1while $\mathbf{B}_2$ is the compatibility matrix for MDS-2. Due to the nonlinear geometry effects, the $\mathbf{B}$ matrix can be highly nonlinear with respect to $\mathbf{q}_1$ and $\mathbf{q}_2$.

Consider, for example, a planar multibody dynamics system, for the $m$th body with generalized coordinates $\mathbf{q}_1^{(m)} = \begin{bmatrix} x_{o_1^{(m)}} & y_{o_1^{(m)}} & \psi_1^{(m)} \end{bmatrix}^T$ in MDS-1, and the $n$th body with generalized coordinates $\mathbf{q}_2^{(n)} = \begin{bmatrix} x_{o_2^{(n)}} & y_{o_2^{(n)}} & \psi_2^{(n)} \end{bmatrix}^T$ in MDS-2. Then the first equation of equations (7) and (8) for the $m$th body in MDS-1 and the $n$th body in MDS-2 can be written in the following Newton-Euler form (Hahn, 2002):

$$\begin{bmatrix} M_1^{(m)} & 0 & 0 \\ 0 & M_1^{(m)} & 0 \\ 0 & 0 & J_1^{(m)} \end{bmatrix} \begin{bmatrix} \ddot{x}_{o_1^{(m)}} \\ \ddot{y}_{o_1^{(m)}} \\ \ddot{\psi}_1^{(m)} \end{bmatrix} = \begin{bmatrix} \sum\limits_{i_m \in I_1^{(m)}} \left(F_{i_m}^{q_1}\right)_x \\ \sum\limits_{i_m \in I_1^{(m)}} \left(F_{i_m}^{q_1}\right)_y \\ \sum\limits_{i_m \in I_1^{(m)}} [-y_{P_{i_m}^{(m)} o_1^{(m)}}^{L_1^{(m)}} \quad x_{P_{i_m}^{(m)} o_1^{(m)}}^{L_1^{(m)}}] \cdot \mathbf{A}^{L_1^{(m)} R} \cdot [\left(F_{i_m}^{q_1}\right)_x \quad \left(F_{i_m}^{q_1}\right)_y]^T \end{bmatrix} + \begin{bmatrix} \left(F_{Ext}^{(m)}\right)_x \\ \left(F_{Ext}^{(m)}\right)_y \\ M_{Ext}^{(m)} \end{bmatrix} \tag{11}$$

$$\begin{bmatrix} M_2^{(n)} & 0 & 0 \\ 0 & M_2^{(n)} & 0 \\ 0 & 0 & J_2^{(n)} \end{bmatrix} \begin{bmatrix} \ddot{x}_{o_2^{(n)}} \\ \ddot{y}_{o_2^{(n)}} \\ \ddot{\psi}_2^{(n)} \end{bmatrix} = \begin{bmatrix} \sum\limits_{i_n \in I_2^{(n)}} \left(F_{i_n}^{q_2}\right)_x \\ \sum\limits_{i_n \in I_2^{(n)}} \left(F_{i_n}^{q_2}\right)_y \\ \sum\limits_{i_n \in I_2^{(n)}} [-y_{Q_{i_n}^{(n)} o_2^{(n)}}^{L_2^{(n)}} \quad x_{Q_{i_n}^{(n)} o_2^{(n)}}^{L_2^{(n)}}] \cdot \mathbf{A}^{L_2^{(n)} R} \cdot [\left(F_{i_n}^{q_2}\right)_x \quad \left(F_{i_n}^{q_2}\right)_y]^T \end{bmatrix} + \begin{bmatrix} \left(F_{Ext}^{(n)}\right)_x \\ \left(F_{Ext}^{(n)}\right)_y \\ M_{Ext}^{(n)} \end{bmatrix} \tag{12}$$

where $M_1^{(m)}$, $M_2^{(n)}$ are the mass of the $m$th body in MDS-1 and the $n$th body in MDS-2. $J_1^{(m)}$ and $J_2^{(n)}$ are the moment of inertia with respect to mass center of the $m$th body and the $n$th body respectively. Assuming there are $N_m$ interaction forces applied on the $m$th body in MDS-1, the indexes of these forces elements are denoted as

$I_1^{(m)} = \left\{ i_1^{(m)} \quad i_2^{(m)} \quad \dots \quad i_{N_m}^{(m)} \right\}$, similarly, for the $n$th body in MDS-2 we can define $I_2^{(n)} = \left\{ i_1^{(n)} \quad i_2^{(n)} \quad \dots \quad i_{N_n}^{(n)} \right\}$. Assuming that the interactive forces apply between the $m$th body in MDS-1 and the $n_1$th body, $n_2$th body, …, $n_{N_m}$th body in MDS-2, then the global force vector for the $m$th body in MDS-1 can be written as $\mathbf{F}_1^{(m)} = \left[ f_{i_1^{(m)}}^{(mn_1)} \quad f_{i_2^{(m)}}^{(mn_2)} \quad \cdots \quad f_{i_{N_m}^{(m)}}^{(mn_{N_m})} \right]^T$ in which $F_{i_m}^{q_1}$ and $F_{i_n}^{q_2}$ are generalized forces of the $i_m$th interactive member for the $m$th body in MDS-1 and the $i_n$th interactive member for the $n$th body in MDS-2, expressed in the global coordinate system. Note that $[-y_{P_{i_m}^{(m)} o_1^{(m)}}^{L_1^{(m)}} \quad x_{P_{i_m}^{(m)} o_1^{(m)}}^{L_1^{(m)}}]$ and $[-y_{Q_{i_n}^{(n)} o_2^{(n)}}^{L_2^{(n)}} \quad x_{Q_{i_n}^{(n)} o_2^{(n)}}^{L_2^{(n)}}]$ are the local position of the $i_m$th attached point $P_{i_m}^{(m)}$ on the $m$th body in MDS-1 and the local position of the $i_n$th attached point $Q_{i_n}^{(n)}$ on the $n$th body in MDS-2. $\left[ \left(F_{Ext}^{(m)}\right)_x \quad \left(F_{Ext}^{(m)}\right)_y \quad M_{Ext}^{(m)} \right]^T$ and $\left[ \left(F_{Ext}^{(n)}\right)_x \quad \left(F_{Ext}^{(n)}\right)_y \quad M_{Ext}^{(n)} \right]^T$ are the external force vectors applied on the respective $m$th body in MDS-1 and $n$th body in MDS-2. $\mathbf{A}^{L_1^{(m)}R}$ and $\mathbf{A}^{L_2^{(n)}R}$ are the transformation matrix between local coordinate system $L_1^{(m)}$, $L_2^{(n)}$ and global coordinates system $R$.

$$\mathbf{A}^{L_1^{(m)}R} = \begin{bmatrix} \cos\psi_1^{(m)} & \sin\psi_1^{(m)} \\ -\sin\psi_1^{(m)} & \cos\psi_1^{(m)} \end{bmatrix} \tag{13}$$

$$\mathbf{A}^{L_2^{(n)}R} = \begin{bmatrix} \cos\psi_2^{(n)} & \sin\psi_2^{(n)} \\ -\sin\psi_2^{(n)} & \cos\psi_2^{(n)} \end{bmatrix} \tag{14}$$

The $i$th interactive force, which connects the $m$th body in MDS-1 and the $n$th body in MDS-2, can be expressed in the global system $R$ as follows,

$$\begin{bmatrix} \left(F_i^R\right)_x^{(mn)} \\ \left(F_i^R\right)_y^{(mn)} \end{bmatrix} = \begin{bmatrix} \dfrac{\left(r_{Q_i^{(n)}P_i^{(m)}}^R\right)_x}{\left\| \mathbf{r}_{Q_i^{(n)}P_i^{(m)}} \right\|} & \dfrac{\left(r_{Q_i^{(n)}P_i^{(m)}}^R\right)_y}{\left\| \mathbf{r}_{Q_i^{(n)}P_i^{(m)}} \right\|} \end{bmatrix}^T f_i^{(mn)} \tag{15}$$

Therefore, the global force vector applied on the $m$th body in MDS-1 can be denoted as $\mathbf{F}_1^{(m)} = \left[ f_{i_1}^{(mn_1)} \quad f_{i_2}^{(mn_2)} \quad \cdots \quad f_{i_{N_m}}^{(mn_{N_m})} \right]^T$ and calculated as:

$$\begin{bmatrix} \sum\limits_{i_m \in I_1^{(m)}} \left( F_{i_m}^{q_1} \right)_x \\ \sum\limits_{i_m \in I_1^{(m)}} \left( F_{i_m}^{q_1} \right)_y \\ \sum\limits_{i_m \in I_1^{(m)}} [-y_{P_{i_m}^{(m)} o_1^{(m)}}^{L_1^{(m)}} \quad x_{P_{i_m}^{(m)} o_1^{(m)}}^{L_1^{(m)}}] \cdot \mathbf{A}^{L_1^{(m)} R} \cdot [\left( F_{i_m}^{q_1} \right)_x \quad \left( F_{i_m}^{q_1} \right)_y ]^T \end{bmatrix} = \left( \mathbf{B}_1^{(m)} \right)^T \begin{bmatrix} f_{i_1^{(m)}}^{(mn_1)} \\ f_{i_2^{(m)}}^{(mn_2)} \\ \vdots \\ f_{i_{N_m}^{(m)}}^{(mn_{N_m})} \end{bmatrix} = \left( \mathbf{B}_1^{(m)} \right)^T \mathbf{F}_1^{(m)} \tag{16}$$

where

$$\mathbf{B}_1^{(m)} = \begin{bmatrix} \dfrac{\left( r_{Q_{i_1^{(m)}}^{(n_1)} P_{i_1^{(m)}}^{(m)}}^R \right)_x}{\left\| \mathbf{r}_{Q_{i_1}^{(n_1)} P_{i_1}^{(m)}} \right\|} & \dfrac{\left( r_{Q_{i_1^{(m)}}^{(n_1)} P_{i_1^{(m)}}^{(m)}}^R \right)_y}{\left\| \mathbf{r}_{Q_{i_1}^{(n_1)} P_{i_1}^{(m)}} \right\|} & \left( \mathbf{r}_{P_{i_1^{(m)}}^{(m)} o_1^{(m)}} \times \mathbf{r}_{Q_{i_1^{(m)}}^{(n_1)} P_{i_1^{(m)}}^{(m)}} \right)_z / \left\| \mathbf{r}_{Q_{i_1^{(m)}}^{(n_1)} P_{i_1^{(m)}}^{(m)}} \right\| \\ \dfrac{\left( r_{Q_{i_2^{(m)}}^{(n_2)} P_{i_2^{(m)}}^{(m)}}^R \right)}{\left\| \mathbf{r}_{Q_{i_2^{(m)}}^{(n_2)} P_{i_2^{(m)}}^{(m)}} \right\|} & \dfrac{\left( r_{Q_{i_2^{(m)}}^{(n_2)} P_{i_2^{(m)}}^{(m)}}^R \right)}{\left\| \mathbf{r}_{Q_{i_2^{(m)}}^{(n_2)} P_{i_2^{(m)}}^{(m)}} \right\|} & \left( \mathbf{r}_{P_{i_2^{(m)}}^{(m)} o_1^{(m)}} \times \mathbf{r}_{Q_{i_2^{(m)}}^{(n_2)} P_{i_2}^{(m)}} \right)_z / \left\| \mathbf{r}_{Q_{i_2^{(m)}}^{(n_2)} P_{i_2^{(m)}}^{(m)}} \right\| \\ \vdots & \vdots & \vdots \\ \dfrac{\left( r_{Q_{i_{N_m}^{(m)}}^{(n_{N_m})} P_{i_{N_m}^{(m)}}^{(m)}}^R \right)}{\left\| \mathbf{r}_{Q_{i_{N_m}^{(m)}}^{(n_{N_m})} P_{i_{N_m}^{(m)}}^{(m)}} \right\|} & \dfrac{\left( r_{Q_{i_{N_m}^{(m)}}^{(n_{N_m})} P_{i_{N_m}^{(m)}}^{(m)}}^R \right)}{\left\| \mathbf{r}_{Q_{i_{N_m}^{(m)}}^{(n_{N_m})} P_{i_{N_m}^{(m)}}^{(m)}} \right\|} & \left( \mathbf{r}_{P_{i_{N_m}^{(m)}}^{(m)} o_1^{(m)}} \times \mathbf{r}_{Q_{i_{N_m}^{(m)}}^{(n_{N_m})} P_{i_{N_m}^{(m)}}^{(m)}} \right)_z / \left\| \mathbf{r}_{Q_{i_{N_m}^{(m)}}^{(n_{N_m})} P_{i_{N_m}^{(m)}}^{(m)}} \right\| \end{bmatrix} \tag{17}$$

The relation between the $m$th compatibility matrix $\mathbf{B}_1^{(m)}$ in MDS-1 and the generalized coordinates $\mathbf{q}_1^{(m)}$ and $\mathbf{q}_2^{(n)}$ are, in general, highly nonlinear.

$$\mathbf{r}_{Q_i^{(n)} P_i^{(m)}} = \begin{bmatrix} \left( r_{Q_i^{(n)} P_i^{(m)}}^R \right)_x \\ \left( r_{Q_i^{(n)} P_i^{(m)}}^R \right)_y \end{bmatrix} = \begin{bmatrix} \cos\psi_2^{(n)} \left( r_{Q_i^{(n)} o_2^{(n)}}^{L_2^{(n)}} \right)_x - \sin\psi_2^{(n)} \left( r_{Q_i^{(n)} o_2^{(n)}}^{L_2^{(n)}} \right)_y + x_{o_2^{(n)}} - \cos\psi_1^{(m)} \left( r_{P_i^{(m)} o_1^{(m)}}^{L_1^{(m)}} \right)_x + \sin\psi_1^{(m)} \left( r_{P_i^{(m)} o_1^{(m)}}^{L_1^{(m)}} \right)_y - x_{o_1^{(m)}} \\ \sin\psi_2^{(n)} \left( r_{Q_i^{(n)} o_2^{(n)}}^{L_2^{(n)}} \right)_y + \cos\psi_2^{(n)} \left( r_{Q_i^{(n)} o_2^{(n)}}^{L_2^{(n)}} \right)_y + y_{o_2^{(n)}} - \sin\psi_1^{(m)} \left( r_{P_i^{(m)} o_1^{(m)}}^{L_1^{(m)}} \right)_x - \cos\psi_1^{(m)} \left( r_{P_i^{(m)} o_1^{(m)}}^{L_1^{(m)}} \right)_y - y_{o_1^{(m)}} \end{bmatrix} \tag{18}$$

Substituting equation (18) into (17), we obtain the nonlinear relation between compatibility matrix and the generalized coordinates.

The nonlinear relation between the deformation of the $i$th connecting member $\Delta_i^{(mn)}$ and the generalized coordinates $\mathbf{q}_1^{(m)} = \left[ x_{o_1^{(m)}} \quad y_{o_1^{(m)}} \quad \psi_1^{(m)} \right]^T$ and $\mathbf{q}_2^{(n)} = \left[ x_{o_2^{(n)}} \quad y_{o_2^{(n)}} \quad \psi_2^{(n)} \right]^T$ is due to the large translation,rotation, and nonlinear geometric properties of dynamics systems. The deformation of the $i$th interactive member attached to the $m$th body in MDS-1 and the $n$th body in MDS-2 is:

$$\Delta_i^{(mn)} = \left\| \mathbf{r}_{Q_i^{(n)} P_i^{(m)}} \right\| - \left\| \mathbf{r}_{Q_i^{(n)} P_i^{(m)}} \right\|_{t=t_0} = \left\| \mathbf{A}^{RL_1^{(m)}} \mathbf{r}^{L_1^{(m)}}_{P_i^{(m)} o_1^{(m)}} + \mathbf{r}^{R}_{o_1^{(m)}} - \mathbf{A}^{RL_2^{(n)}} \mathbf{r}^{L_2^{(n)}}_{Q_i^{(n)} o_2^{(n)}} - \mathbf{r}^{R}_{o_2^{(n)}} \right\| - l_i^0 \quad (19)$$

Then, the deformation vector $\mathbf{\Delta}^{(m)}$ for the $m$th body is denoted as

$$\mathbf{\Delta}^{(m)} = \left\{ \Delta_{i_1^{(m)}}^{(mn_1)} \quad \Delta_{i_2^{(m)}}^{(mn_2)} \quad \cdots \quad \Delta_{i_{N_m}^{(m)}}^{(mn_{N_m})} \right\}^T \quad (20)$$

The following relationship is obtained between the $m$th deformation vector $\mathbf{\Delta}^{(m)}$ and the $m$th compatibility matrix $\mathbf{B}_1^{(m)}$ by differentiating equation (20) with respect to the generalized coordinates:

$$\frac{\partial \mathbf{\Delta}^{(m)}}{\partial \mathbf{q}_1^{(m)}} = \begin{bmatrix} \dfrac{\partial \Delta_{i_1^{(m)}}^{(mn_1)}}{\partial x_{o_1^{(m)}}^R} & \dfrac{\partial \Delta_{i_1^{(m)}}^{(mn_1)}}{\partial y_{o_1^{(m)}}^R} & \dfrac{\partial \Delta_{i_1^{(m)}}^{(mn_1)}}{\partial \psi_1^{(m)}} \\ \dfrac{\partial \Delta_{i_2^{(m)}}^{(mn_2)}}{\partial x_{o_1^{(m)}}^R} & \dfrac{\partial \Delta_{i_2^{(m)}}^{(mn_2)}}{\partial y_{o_1^{(m)}}^R} & \dfrac{\partial \Delta_{i_2^{(m)}}^{(mn_2)}}{\partial \psi_1^{(m)}} \\ \vdots & \vdots & \vdots \\ \dfrac{\partial \Delta_{i_{N_m}^{(m)}}^{(mn_{N_m})}}{\partial x_{o_1^{(m)}}^R} & \dfrac{\partial \Delta_{i_{N_m}^{(m)}}^{(mn_{N_m})}}{\partial y_{o_1^{(m)}}^R} & \dfrac{\partial \Delta_{i_{N_m}^{(m)}}^{(mn_{N_m})}}{\partial \psi_1^{(m)}} \end{bmatrix} = -\mathbf{B}_1^{(m)} \quad (21)$$

## 3 Design variables in the optimization problem

The optimization problem is defined based on state equations, general force elements and critical boundary conditions. The design variables in this work, $\boldsymbol{\alpha} = [\alpha_1 \quad \alpha_2 \quad \cdots \quad \alpha_N]^T$, $0 \le \alpha_i \le 1 \ (i = 1, 2, \dots, N)$, are similar to the relative density design variables in power-law approach or SIMP method, and are associated with each original global force element $f_i$. The design variables vector $\boldsymbol{\alpha}$ also could be defined as cost functions or material coefficients. The modified global force element in the optimization problem $f_i^*$ is written as:

$$f_i^* = \alpha_i^\mu f_i \quad \left(0 \le \alpha_i \le 1,\ i = 1, 2, \ldots, N\right) \tag{22}$$

where $\mu$ is the power parameter

The global force vector $\mathbf{F}$ including design variables will be rewritten as follows:

$$\mathbf{F} = \left[ \alpha_1^\mu f_1 \quad \alpha_2^\mu f_2 \quad \cdots \quad \alpha_N^\mu f_N \right]^T \tag{23}$$

## 4 Topology optimization for multidisciplinary structure design

In general, an objective function for multibody dynamics systems can be written as a function of generalized coordinates, generalized velocities and generalized accelerations, namely, $g = g(\mathbf{q}, \dot{\mathbf{q}}, \ddot{\mathbf{q}}, \boldsymbol{\alpha})$. The topology optimization for multibody dynamics systems with multidisciplinary structural components with respect to dynamic response has a general form:

$$\begin{aligned}
&\min_{\boldsymbol{\alpha}} g(\mathbf{q}, \dot{\mathbf{q}}, \ddot{\mathbf{q}}, \boldsymbol{\alpha}) \\
&s.t.: \qquad \text{state equations} \\
&\qquad \sum_{i=1}^{P} \gamma_i^j \alpha_i V_i \le h_{0j} \quad \left( j = 1, 2, \ldots, M \right) \\
&\qquad 0 \le \underline{\alpha}_i \le \alpha_i \le \overline{\alpha}_i \le 1 \quad \left(i = 1, 2, \ldots, N\right) \\
&\qquad \gamma_i^j : \text{grouping index } \left(\gamma_i^j = 0 \text{ or } 1\right)
\end{aligned} \tag{24}$$

where $M$ is the total number of constraints, $V_i$ is the volume or cost function for the $i$th constraint. The components in the restraint system can be divided into different groups, which may belong to different disciplines, and each group can have its own constraint, resulting in a multi-constraint design problem. Figure 2 shows the flow chart of the multidisciplinary structure design process.

**Figure2** Multidisciplinary structure optimization process

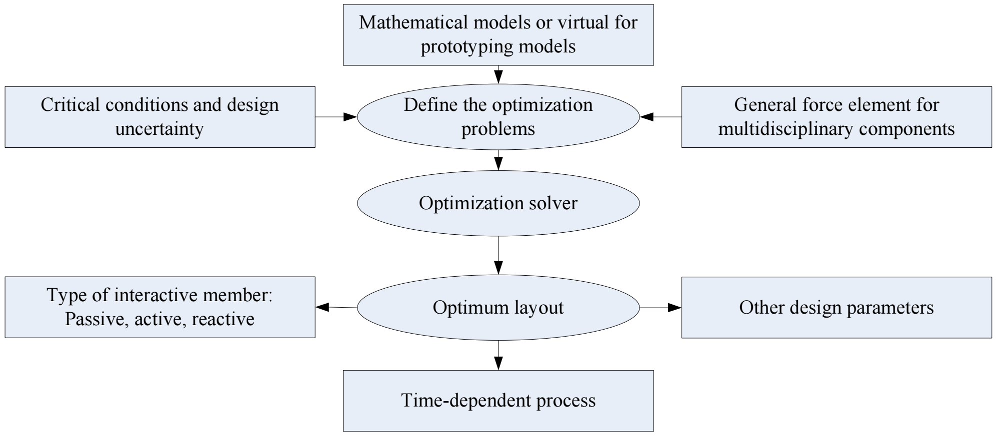


*4.1 Optimization algorithm*

The Generalized Sequential Approximate Optimization (GSAO) developed by Ma and Kikuchi (1995a) is adopted to solve this topology optimization problem. This algorithm, based on convex approximation, extends the compatibility of previous optimization algorithms significantly by using advanced updating rules and offering more appropriate parameters for the optimization process algorithm. In specific cases, this algorithm reduces to most popular topology algorithms, such as OC, COLIN, MMA, DSPQ and MOC. The GSAO enhancements result in improved convergence, higher computational efficiency and a more stabile iterative process for large-scale optimization problems. GSAO also is well suited for multi-constraint problems. The flow chart of the GASO optimization process is shown in Figure 3.

**Figure3** Flow chart of GSAO optimization process

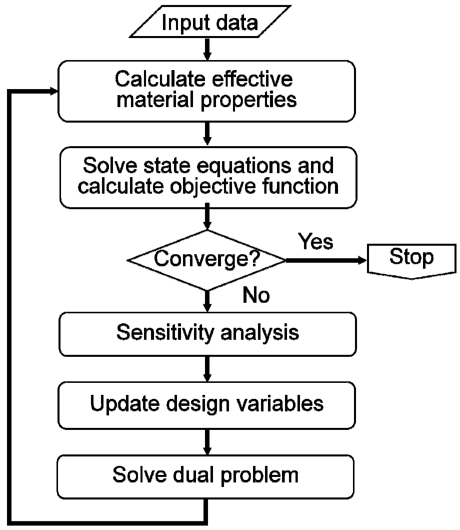


Using the GASO algorithm, a sequence of approximate optimization problems is obtained:

$$\begin{aligned}
&\text{minimize } \; g_0^k + \sum_{i=1}^{n} a_i^k \left|\alpha_i - c_i\right|^{\xi_i} \\
&h_{0j}^k + \sum_{i=1}^{n} b_{ji}^k \left|\alpha_i - e_{ji}\right|^{\zeta_{ji}} \le 0 \quad \left(j = 1, 2, \ldots, m\right) \\
&\underline{\alpha}_i \le \alpha_i \le \overline{\alpha}_i \quad \left(i = 1, 2, \ldots, N\right)
\end{aligned} \tag{25}$$

By properly choosing the optimization parameter, the approximate optimization problem can always be made convex. It is then solved by using the dual method, where the dual problem is given by

$$\begin{aligned}
&\underset{\boldsymbol{\lambda}}{\text{maximize}} \; L^k(\mathbf{X}^*(\boldsymbol{\lambda}), \boldsymbol{\lambda}) \\
&\lambda_j > 0 \quad \left(j = 1, 2, \ldots, m\right)
\end{aligned} \tag{26}$$

A typical updating rule for the GSAO method is:

$$\alpha_i^* = c_i + \left( -\frac{g_{,\alpha_i}^k}{\sum_{j=1}^{m} \lambda_j h_{j,\alpha_i}^k} \right)^{\eta_i} \left( \alpha_i^k - c_i \right) \quad (i = 1, 2, \ldots, N) \tag{27}$$

*4.2 Sensitivity analysis*

Combining equations (7), (8), and (10):

$$\begin{cases} \mathbf{M}(\mathbf{q})\ddot{\mathbf{q}} - \mathbf{Q} + \left(\mathbf{C}\right)_{\mathbf{q}}^T \boldsymbol{\lambda} = \mathbf{F}^{Ext} + \mathbf{B}^T \mathbf{F} \\ \mathbf{C}\left(\mathbf{q}, \dot{\mathbf{q}}\right) = \mathbf{0} \end{cases} \tag{28}$$

where,

$$\mathbf{q} = \begin{bmatrix} \mathbf{q}_1 \\ \mathbf{q}_2 \end{bmatrix}, \quad \mathbf{M} = \begin{bmatrix} \mathbf{M}_1 & 0 \\ 0 & \mathbf{M}_2 \end{bmatrix}, \quad \mathbf{Q} = \begin{bmatrix} \mathbf{Q}_1 \\ \mathbf{Q}_2 \end{bmatrix}, \quad \left(\mathbf{C}\right)_{\mathbf{q}} = \begin{bmatrix} \left(\mathbf{C}_1\right)_{\mathbf{q}_1} & 0 \\ 0 & \left(\mathbf{C}_2\right)_{\mathbf{q}_2} \end{bmatrix},$$
$$\boldsymbol{\lambda} = \begin{bmatrix} \boldsymbol{\lambda}_1 \\ \boldsymbol{\lambda}_2 \end{bmatrix}, \quad \mathbf{F}^{Ext} = \begin{bmatrix} \mathbf{F}_1^{Ext} \\ \mathbf{F}_2^{Ext} \end{bmatrix} \text{ and } \mathbf{C} = \begin{bmatrix} \mathbf{C}_1 \\ \mathbf{C}_2 \end{bmatrix} \tag{29}$$

To simplify the discussion of the sensitivity analysis in this section, it is assumed that the global force vector $\mathbf{F}$ in equation (28) is only an explicit function of the deformation vector $\boldsymbol{\Delta}$ and the design variables $\boldsymbol{\alpha}$, namely

$$\mathbf{F} = \mathbf{F}(\boldsymbol{\Delta},\ \boldsymbol{\alpha}) \tag{30}$$

While a more accurate sensitivity analysis method can be obtained, we propose a simplified but efficient sensitivity analysis method, which can be easily implemented into commercial multibody dynamics codes, such as MSC/ADAMS.

The first equation in equation (28) can be rewritten as

$$\mathbf{F}^q = \mathbf{M}(\mathbf{q})\ddot{\mathbf{q}} - \mathbf{Q} + \left(\mathbf{C}\right)_{\mathbf{q}}^T \boldsymbol{\lambda} - \mathbf{F}^{Ext} = \mathbf{B}^T \mathbf{F} \tag{31}$$

Here $\mathbf{F}^q$ is the generalized action-reaction force between the multibody dynamics system and the restraint system. Since the objective is to obtain an optimal restraint system, the parameters in the two given multibody dynamics systems are not allow to change. To apply the simplified sensitivity analysis method, it is assumed that $\mathbf{F}^q = \mathbf{F}^q(t)$ in equation (31) is the force obtained in the previous design stage by solving equation (28), but it is a given force when evaluating the design changes at the current stage. This assumption significantly simplifies the sensitivity analysis process.

Taking the derivative of equation (31):

$$\mathbf{0} = \left(\frac{d\mathbf{B}}{d\boldsymbol{\alpha}}\right)^T \mathbf{F} + \mathbf{B}^T \left(\frac{d\mathbf{F}}{d\boldsymbol{\alpha}}\right) \tag{32}$$

Similarly from equation (30):

$$\frac{d\mathbf{F}}{d\boldsymbol{\alpha}} = \frac{\partial \mathbf{F}}{\partial \boldsymbol{\Delta}} \frac{\partial \boldsymbol{\Delta}}{\partial \mathbf{q}} \frac{d\mathbf{q}}{d\boldsymbol{\alpha}} + \frac{\partial \mathbf{F}}{\partial \boldsymbol{\alpha}} = -\mathbf{K}\mathbf{B}\frac{d\mathbf{q}}{d\boldsymbol{\alpha}} + \frac{\partial \mathbf{F}}{\partial \boldsymbol{\alpha}} \tag{33}$$

and by application of the chain rule:

$$\frac{d\mathbf{B}}{d\boldsymbol{\alpha}} = \frac{\partial \mathbf{B}}{\partial \mathbf{q}} \frac{d\mathbf{q}}{d\boldsymbol{\alpha}} \tag{34}$$

where $\mathbf{K} = \frac{\partial \mathbf{F}}{\partial \boldsymbol{\Delta}}$ and $\mathbf{B} = -\frac{\partial \boldsymbol{\Delta}}{\partial \mathbf{q}}$.

Substituting equations (33) and (34) into equation (32):

$$\left(\mathbf{B}^T\mathbf{K}\mathbf{B} - \mathbf{F}^T \frac{\partial \mathbf{B}}{\partial \mathbf{q}}\right)\frac{d\mathbf{q}}{d\boldsymbol{\alpha}} = \mathbf{B}^T \frac{\partial \mathbf{F}}{\partial \boldsymbol{\alpha}} \tag{35}$$

which can be solved as:

$$\frac{d\mathbf{q}}{d\boldsymbol{\alpha}} = \left(\mathbf{B}^T\mathbf{K}\mathbf{B} - \mathbf{F}^T \frac{\partial \mathbf{B}}{\partial \mathbf{q}}\right)^{-1} \mathbf{B}^T \frac{\partial \mathbf{F}}{\partial \boldsymbol{\alpha}} \tag{36}$$

In general, assuming objective function $g = g(\mathbf{q}, \boldsymbol{\alpha})$ is a function of generalized coordinates $\mathbf{q}$ and design variable vector $\boldsymbol{\alpha}$, then we have

$$\frac{dg}{d\boldsymbol{\alpha}} = \frac{\partial g}{\partial \mathbf{q}}\frac{d\mathbf{q}}{d\boldsymbol{\alpha}} + \frac{\partial g}{\partial \boldsymbol{\alpha}} = \frac{\partial g}{\partial \mathbf{q}}\left(\mathbf{B}^T\mathbf{K}\mathbf{B} - \mathbf{F}^T\frac{\partial \mathbf{B}}{\partial \mathbf{q}}\right)^{-1}\mathbf{B}^T\frac{\partial \mathbf{F}}{\partial \boldsymbol{\alpha}} + \frac{\partial g}{\partial \boldsymbol{\alpha}} \tag{37}$$

Adopting an adjoint vector $\mathbf{v}$, which satisfies the following adjoint equation:

$$\left(\mathbf{B}^T\mathbf{K}\mathbf{B} - \mathbf{F}^T\frac{\partial \mathbf{B}}{\partial \mathbf{q}}\right)\mathbf{v} = \left(\frac{\partial g}{\partial \mathbf{q}}\right)^T \tag{38}$$

we have

$$\frac{dg}{d\boldsymbol{\alpha}} = \mathbf{v}^T\mathbf{B}^T\frac{\partial \mathbf{F}}{\partial \boldsymbol{\alpha}} + \frac{\partial g}{\partial \boldsymbol{\alpha}} \tag{39}$$

For the special case where $\mathbf{F} = \mathbf{K}\boldsymbol{\Delta}$ and $\mathbf{K} = \mathbf{K}(\boldsymbol{\alpha})$, we will have

$$\frac{dg}{d\boldsymbol{\alpha}} = \mathbf{v}^T\left(\mathbf{B}^T\frac{\partial \mathbf{K}}{\partial \boldsymbol{\alpha}}\boldsymbol{\Delta}\right) + \frac{\partial g}{\partial \boldsymbol{\alpha}} \tag{40}$$

In general case, $\mathbf{F}$ can be a nonlinear function of $\boldsymbol{\Delta}$, but equation (39) still holds.

*4.3 Reverse method for compatibility matrix calculation*

Generally, the compatibility matrix **B** is difficult to obtain, particularly if the internal information of a multibody dynamics code is not accessible. There is a need to develop a more effective calculation method to obtain the **B** matrix using only the information available during a normal solution process without requiring internal information or modifying the multibody dynamics code. In general, the compatibility matrix **B** is the assembly matrix of the sub-matrices $\mathbf{B}^{(i)}$ where $\mathbf{B}^{(i)} = -\frac{\partial \boldsymbol{\Delta}^{(i)}}{\partial \mathbf{q}^{(i)}}$ and $\mathbf{q}^{(i)}$ is the generalized coordinate vector of the *i*th body in the multibody system and $\boldsymbol{\Delta}^{(i)}$ is the displacement vector associated with the $i$th body. Assume that $\mathbf{B}_n^{(i)}$ denotes the compatibility matrix $\mathbf{B}^{(i)}$ at the $n_{th}$ time step, and $\mathbf{\Delta}_n^{(i)}$ is the corresponding displacement at the $n_{th}$ time step. Then, using the first order Taylor expansion of $\mathbf{\Delta}_n^{(i)}$ at a point $\mathbf{q}_0^{(i)}$ near to $\mathbf{q}_n^{(i)}$ :

$$\mathbf{\Delta}_n^{(i)} = \mathbf{\Delta}_0^{(i)} + \frac{\partial \mathbf{\Delta}_n^{(i)}}{\partial \mathbf{q}^{(i)}} \left( \mathbf{q}_n^{(i)} - \mathbf{q}_0^{(i)} \right) = \mathbf{\Delta}_0^{(i)} - \mathbf{B}_n^{(i)} \left( \mathbf{q}_n^{(i)} - \mathbf{q}_0^{(i)} \right) \tag{41}$$

or

$$\mathbf{B}_n^{(i)} \left( \mathbf{q}_n^{(i)} - \mathbf{q}_0^{(i)} \right) = \mathbf{\Delta}_0^{(i)} - \mathbf{\Delta}_n^{(i)}$$

Using the same process, for the time steps $n+j$ ( $j = 1, 2, \ldots, j_n$ ) , we obtain

$$\mathbf{B}_{n+j}^{(i)} \left( \mathbf{q}_{n+j}^{(i)} - \mathbf{q}_0^{(i)} \right) = \mathbf{\Delta}_0^{(i)} - \mathbf{\Delta}_{n+j}^{(i)} \tag{42}$$

where, for the two-dimensional system $j_n = 3$ and for the three-dimensional system $j_n = 6$ .

Since $\mathbf{\Delta}_n^{(i)}$ and $\mathbf{q}_n^{(i)}$ are calculated at each time step, by assuming the compatibility matrix is constant within the small time interval, we obtain

$$\mathbf{B}_n^{(i)} \left[ \mathbf{q}_{n+1}^{(i)} - \mathbf{q}_0^{(i)}, \ldots, \mathbf{q}_{n+j_n}^{(i)} - \mathbf{q}_0^{(i)} \right] = \left[ \mathbf{\Delta}_0^{(i)} - \mathbf{\Delta}_{n+1}^{(i)}, \ldots, \mathbf{\Delta}_0^{(i)} - \mathbf{\Delta}_{n+j_n}^{(i)} \right] \tag{43}$$

Equation (43), can be solved for $\mathbf{B}_n^{(i)}$ . By assembling all $\mathbf{B}_n^{(i)}$ the global $\mathbf{B}$ matrix is constructed.

*4.4 Numerical example for a two rigid body dynamics system*

A two rigid body dynamics system is shown in Figure 4, with the mass of body 1 = 60 $kg$ and its mass moment of inertia = 10 $kg \cdot m^2$; and the mass of body 2 = 2,000 $kg$ , and its mass moment of inertia = 1.0E6 $kg \cdot m^2$ . There are 51 connecting members each with initial linear stiffness = 200 N/m. An angular acceleration is applied to body 2 of magnitude 10 $rad/s^2$ with the rotation center of $O_2$.

**Figure 4** Two rigid bodies dynamics model

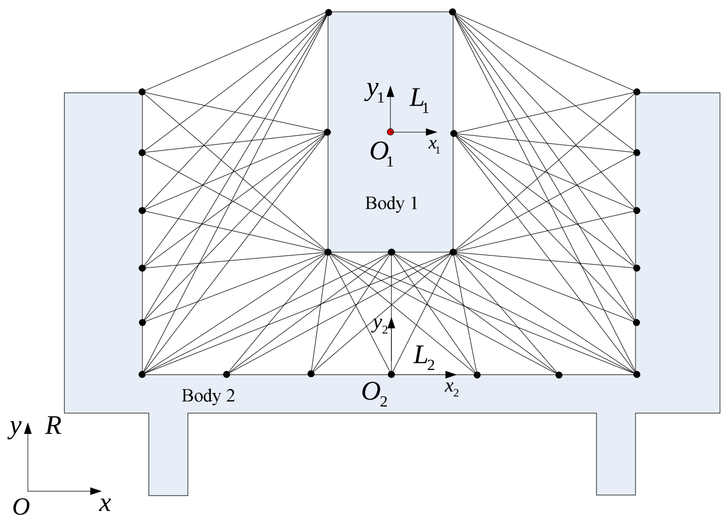


Consider an objective function as the maximum relative translation displacement of body 1 with respect to body 2, and the optimization problem is to minimize the objective function. The objective function is defined as follows:

$$\min_{\alpha_i\,(i=1,2,\ldots,N)}\left\{\max_{[t_0,t_1]} g=\left[\mathbf{A}^{L_2R}\left(\mathbf{q}^1-\mathbf{q}^2\right)-\mathbf{r}_{O_1O_2}^{L_2}\Big|_{t=t_0}\right]^T\mathbf{W}\left[\mathbf{A}^{L_2R}\left(\mathbf{q}^1-\mathbf{q}^2\right)-\mathbf{r}_{O_1O_2}^{L_2}\Big|_{t=t_0}\right]\right\} \tag{44}$$

where $\mathbf{q}^1=\begin{bmatrix}x_{O_1} & y_{O_1} & \psi_1\end{bmatrix}^T$, $\mathbf{q}^2=\begin{bmatrix}x_{O_2} & y_{O_2} & \psi_2\end{bmatrix}^T$, are generalized coordinates body 1 and 2, respectively; $\mathbf{A}^{L_2R}$ is the transformation matrix from global coordinate system $R$ to local coordinate system $L_2$. $\mathbf{r}_{O_1O_2}^{L_2}\Big|_{t=t_0}$ is the vector $\mathbf{r}_{O_1O_2}$ in local coordinate system at the initial time , and $\mathbf{W}$ is a weighting matrix, assumed as $\mathbf{W}=\begin{bmatrix}1 & & \\ & 1 & \\ & & 0\end{bmatrix}$.

**Figure 5** Two rigid body dynamics system optimization result

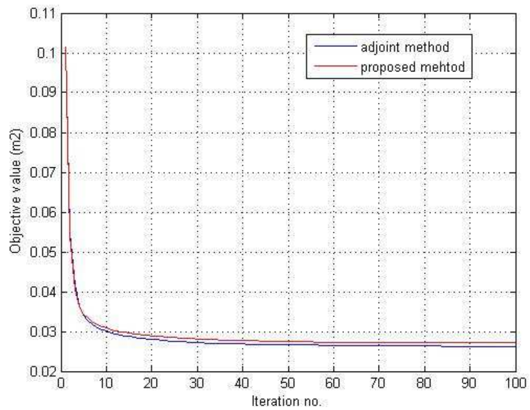


Both a traditional adjoint method and the proposed sensitivity analysis method were used to solve the example problem. From Figure 5, it can be seen that the adjoint method converges to an optimization result of 0.026 $m^2$; the proposed method converges to an optimization result of 0.027 $m^2$. It is well known that computing sensitivities using a finite difference method requires unacceptably long computation times for a large number of design variables. Using the adjoint method, it was necessary to solve another set of differential-algebraic equations. The proposed method calculates the sensitivities based only on a single computation of the multibody dynamics simulation. Moreover using the reverse compatibility matrix method reduces the complexity of the sensitivity calculation significantly. Therefore, the optimization problem can be solved efficiently to achieve acceptable accuracy.

## 5 Application to vehicle occupant restraint systems

One important application of the multidisciplinary structure design methodology is to design a vehicle occupant restraint system to improve the occupants' safety. The restraint system should also help stabilize the occupant over rough terrain and high speed maneuver conditions and needs to be user friendly, such as easy to put on and take off. The restraint system involves a possible usage of passive, active, and other reactive devices, and these multidisciplinary safety elements such as belts, airbags or retractors have to be activated in a specific sequence and timing to protect the occupant in extreme conditions. Minimizing the system weight, cost and complexity are also considered in design process. Therefore, it is necessary to develop a general and systematic design approach and optimization tool, which can enlarge the design space and obtain optimal layout design for best performance/weight and performance/cost ratios. Traditional design solution based on engineers' intuition may not provide the best combination of functionality.

Virtual prototyping multibody dynamics models are developed for computational simulation in a commercial code. The detailed specification of a virtual 24-years old male occupant multibody dynamics model (Figure 6) is listed in Table 1.

**Figure 6** The occupant model

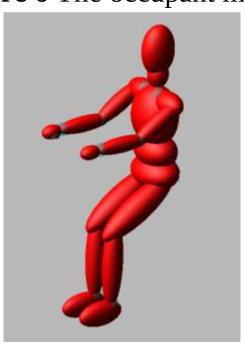

**Table 1** Specifications of occupant model

| | |
|---|---|
| Weight | 77 Kg |
| Height | 1.778 m |
| CGX ( +: rearward from the front axial) | 1.848 m |
| CGY (+: rightward from midplane) | 0.041 m |
| CGZ (+: upward from the ground) | 1.758 m |
| Part number | 58 |

There are three connecting bushings created for integrating the occupant and vehicle model together (Figure 7). Two bushings connect the occupant's hands with the vehicle, and one bushing connects the occupant's lower torso with the seat on the vehicle to simulate the occupant's sitting posture. The detailed specifications of the integrated model are given in Table 2. The joint stiffness properties of the occupant are based on the data measured from a Hybrid III dummy finite element model in a software library and biomechanical publications (Dhaher et al., 2005, Dinant and Kistemaker, 2007; Granata et al., 2004; Gunther and Blickhan, 2002; Leger and Milner, 2000; LSTC, 2007; Magnusson, 1988, Van der Spek et al., 2003; Xu, 1999).

**Figure 7** Integrated occupant and vehicle model

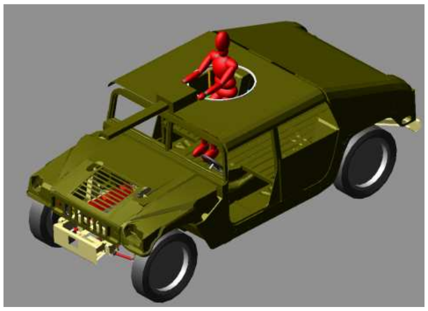

**Table 2** Specifications of integrated model

| | |
|---|---|
| Weight | 2898 Kg |
| CGX ( +: rearward from the front axial) | 1.70 m |
| CGY (+: rightward from midplane) | 0.0006 m |
| CGZ (+: upward from the ground) | 0.80 m |
| Part number | 128 |

Three virtual proving grounds were employed for this study: severe braking, rollover and rough terrains. For the severe braking case, the initial vehicle longitudinal velocity is 17 m/s, and the vehicle deceleration is 9.8 $m/s^2$. For the rollover case, the initial vehicle longitudinal velocity is 17 m/s, and the steering wheel rotates 720° in 1 second for the vehicle system. For the rough terrain case, the initial vehicle longitudinal velocity is 17 m/s, and the road profile is a sinusoid function with magnitude of 0.05 m and wave length of 8 m.

Critical conditions for the design problem were identified and design uncertainties were eliminated, including the effect of the gunner's awareness in terms of hand grasping: i) gunner intentionally grasps the handle in a maneuver; ii)and gunner does not grip handle in a maneuver; the effect of hand gripping strength with a stronger gunner and a weaker occupant; the effect of joint stiffness where the gunner intentionally holds the position or the gunner is in the relaxed condition; the effect of terrain roughness with rough terrain and flatter terrain; the effect of gunner postures considering seated and standing postures with different orientations. Detailed results can be found in Dong et al. (2009) and Ma et al. (2010). As an example of these studies to identify critical conditions, consider of the gunner's center of gravity (CG) height with respect to the vehicle's roof, as shown in Figure 8 and Figure 9. The gunner is ejected during severe braking if the gunner's hands are not grasping anything on the vehicle, but remains in the crew compartment in hands grasping case. It is concluded that the condition of hands free grasping is more critical in the restraint system design.

**Figure 8** Occupant CG relative height response with different grasping condition in brake

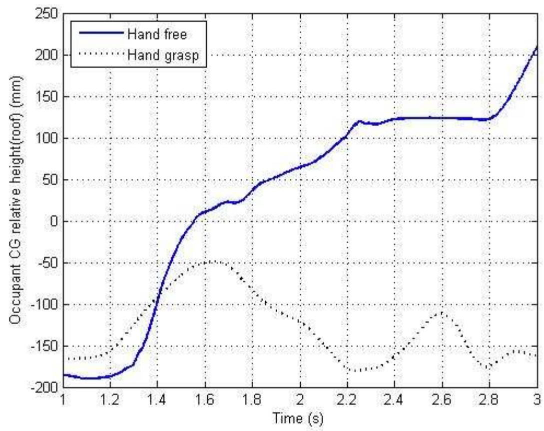


**Figure 9** Occupant response in brake condition at 3s (a) hand free (b) hand grasping

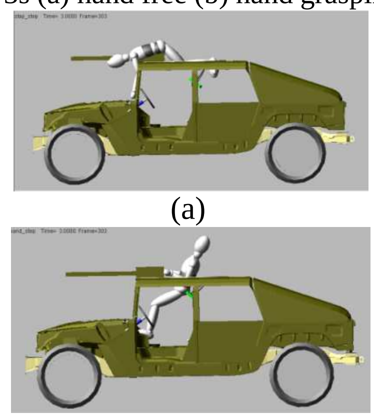

(a)

(b)

The initial design space was set up with evenly distributed connecting members with linear stiffness in all possible connections. In order to discretize the design space, as shown in Figure 10, 5 vertical layers of connection nodes were placed on the vehicle, 22 predetermined connection nodes on the occupant, resulting in 580 connection members between the gunner and the vehicle. The function-oriented multidisciplinary structure optimization was employed to optimize the geometrically nonlinear, time-dependent structural/multibody dynamics system based on the connectivity of interaction points on occupant and vehicle, optimal interaction members and optimal physical properties of the interaction members for occupant at vehicle. The optimal structure layout was obtained by removing unnecessary connecting members and reinforcing necessary connecting members via the optimization algorithm. Critical for the optimization was the use of the proposed sensitivity calculation to efficiently address the nonlinear geometry effects and large motion in dynamic response optimization.

**Figure 10** Initial structural universe with connecting points on (a) vehicle and (b) occupant

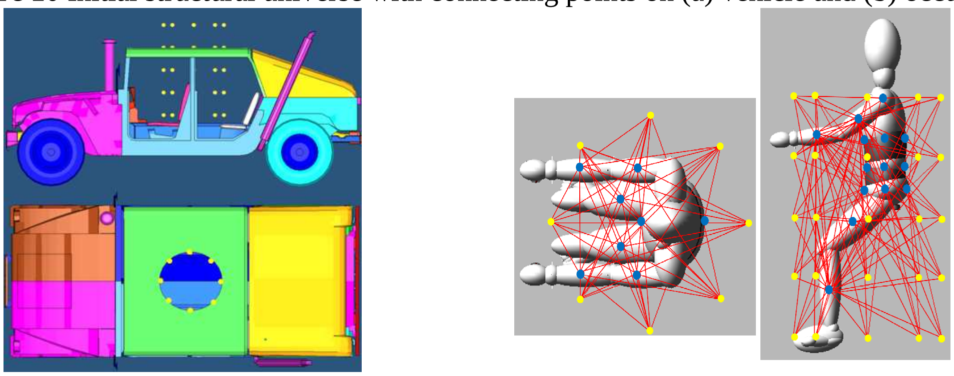

(a) (b)

Every connecting member was associated with a material coefficient, $0 \le \alpha_i \le 1$ for the $i_{th}$ member, and it was assumed that stiffness is proportional with this material coefficient, so the stiffness assigned for the $i_{th}$ connecting member is $\alpha_i k_0$. Consequently, $\alpha_i = 0$ means this member should be removed in the layout, and $\alpha_i = 1$ means this member should remain.

The flow chart in Figure 11 shows the optimization process applied for an occupant restraint system optimization design, which was implemented by coupling the commercial codes.

**Figure 11** Flow chart of multidisciplinary structure optimization process

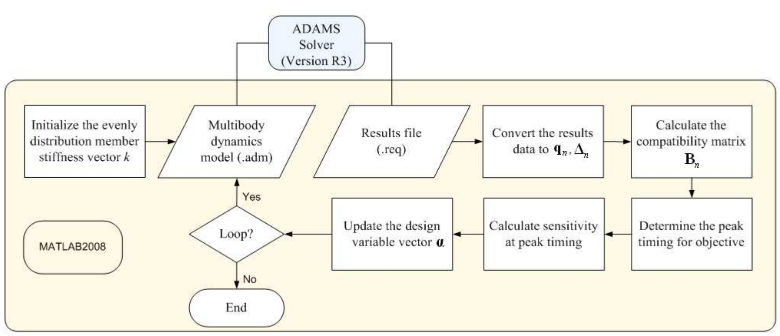


 UNCLASSIFIED

In order to avoid an physically infeasible and expensive restraint system, the design space was reduced to only keeping 180 connecting members between the gunner's upper torso, central torso, lower torso and vehicle body for the preliminary study. The maneuver condition for the vehicle is a step steer condition, in which the steering wheel rotates 360$^{o}$ in 0.5 seconds with initial longitudinal velocity of 17m/s. The objective function is defined as the maximum relative translation displacement between the gunner's center of gravity and the vehicle in the time duration $[t_0, t_1]$, and design objective is to minimize the maximum relative translation displacement as defined in equation (45)

$$\min_{\alpha_i\,(i=1,2,\ldots,N)} \left\{ \max_{[t_0,t_1]} g = \left[ \mathbf{A}^{L_V R}\left(\mathbf{q}^{O} - \mathbf{q}^{V}\right) - \mathbf{r}^{L_V}_{O_O O_V}\Big|_{t=t_0} \right]^T \mathbf{W} \left[ \mathbf{A}^{L_V R}\left(\mathbf{q}^{O} - \mathbf{q}^{V}\right) - \mathbf{r}^{L_V}_{O_O O_V}\Big|_{t=t_0} \right] \right\} \qquad (45)$$

where $\mathbf{q}^{O}, \mathbf{q}^{V}$ are the respective generalized coordinates for the gunner's center of gravity and vehicle body, and $\mathbf{W} = \begin{bmatrix} \mathbf{I}_{3\times3} & \mathbf{0} \\ \mathbf{0} & \mathbf{0} \end{bmatrix}$

Figure 12 shows the design objective. From the design objective iteration results in Figure 12 (a), it is concluded that the proposed function-oriented design method based on topology optimization can solved the problem appropriately and also reduce the maximum occupant relative translation displacement with respect to the vehicle with fewer active connecting members. That is, the active remaining members can restrain the occupant at the initial position more effectively than the initial evenly distributed members. In Figure 12 (b), the black color denotes a higher value of design variable, i.e., the member should remain in the final layout; while the grey color means a medium value of design variable, or the members need more investigation and the white color means a lower value of design variable, or the members can be removed in the final layout.

**Figure 12**. Optimization iteration results (a) and interactive members' final stiffness distribution (b)

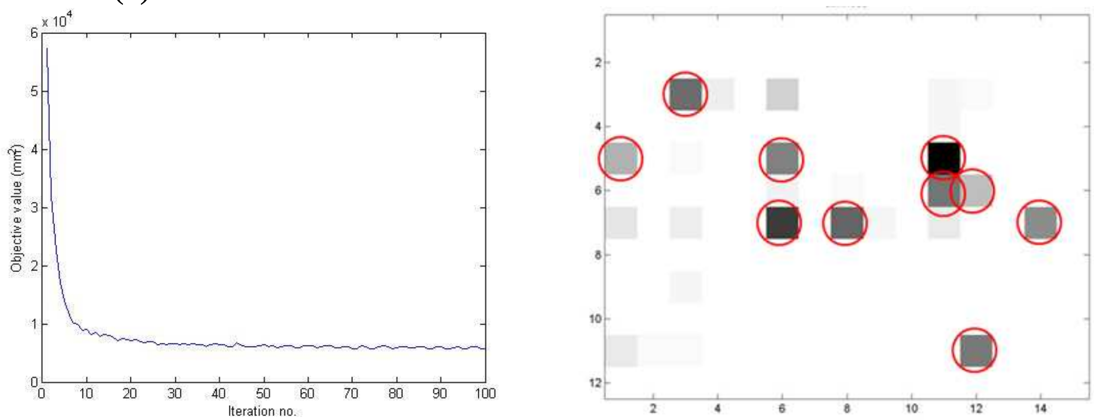


(a) (b)

Figure 13 shows the gunner's dynamic response under the step steer condition. The upper row is the dynamic response before optimization, in which all the interactive members' stiffness was distributed evenly; the lower row is after optimization, with stiffness distributed as shown in Figure 12 (b). From the rightmost frames, it is obvious that the optimized interactive members layout can constrain the occupant much more effectively in dynamic loading condition with same total stiffness amount.

**Figure 13**. Occupant dynamic response in (a)0.25s (b)0.5s (c)0.75s and (d) 1s

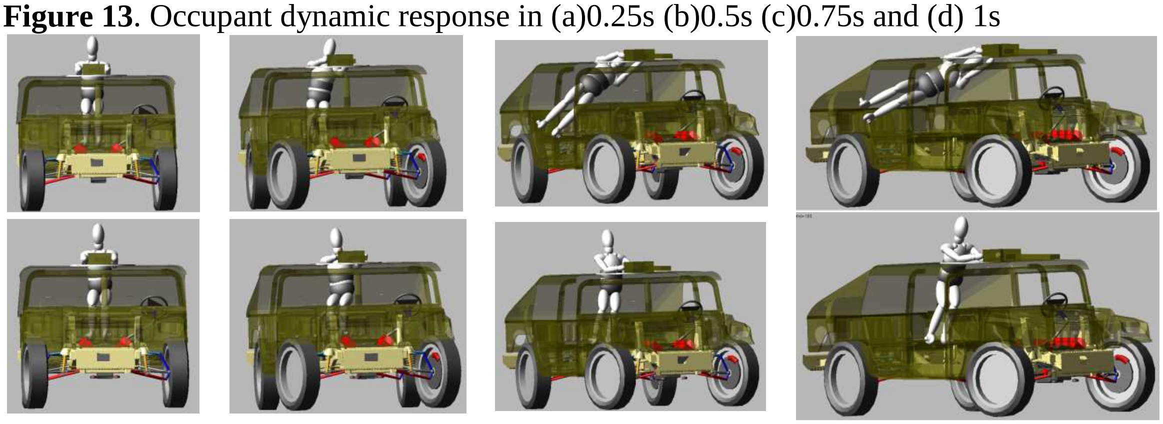

(a) 0.25s (b) 0.5s (c) 0.75s (d) 1s

Further interpretation of the optimum layout depends on the mechanical properties of the remaining connecting members and the engineer's intuition. If deformation of remaining members is further investigated, the compression members, which are shown as (-), can be realized as airbag devices and the tension members, which are shown as (+), could be realized as belt devices in further components design based on Figure 14.

**Figure 14**. Optimum connecting members layout

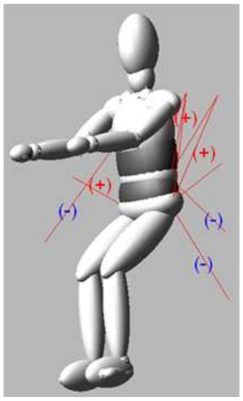


The ordinary linear stiffness members in the multibody dynamics system can also be substituted with connecting members with nonlinear stiffness, such as shown in Figure 15. Using this nonlinear stiffness response, the optimized result under the step steer condition is shown in Figure 16, and it is concluded that the proposed function-oriented design method based on topology optimization can also be applied to the system design with nonlinear interactive members.

**Figure 15.** Interactive members' nonlinear stiffness

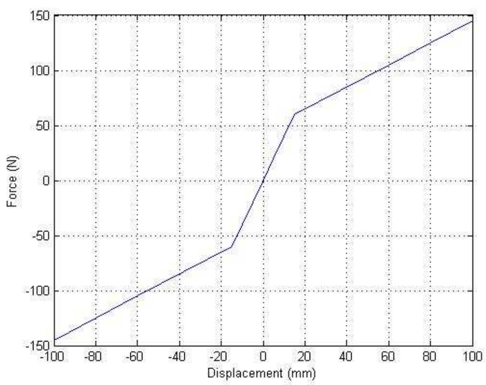


**Figure 16.** Nonlinear members' optimization results

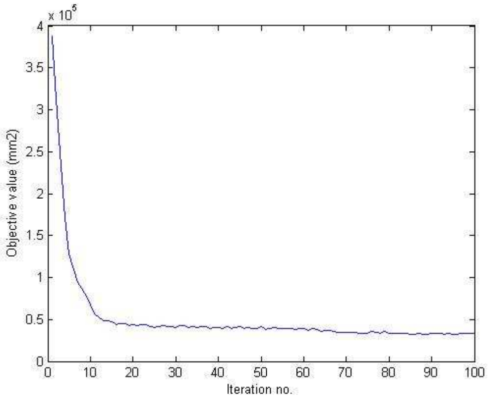

## 6 Critical parameters identification for multidisciplinary components design

Once obtaining an optimum layout using the proposed general multidisciplinary structure function-oriented design method, it is necessary to identify the type of interactive members, such as passive, active, reactive, and to identify timing parameters, length of actuation period or other effective design variables, such as critical design parameters of mechanical properties for different components. To do so, various nonlinear general force (G-force) elements need to be developed to represent multidisciplinary components, and then be incorporated into the design problem.

As an example, consider a belt retractor design, in which the number of retractors, single point or multiple points; location of the connecting points, both on the occupant and on the vehicle are obtained in the final optimum layout design using the proposed method. Critical design parameters for properties of the retractor need to be identified in next step. A series of five bench-top retractor tests were conducted by Newberry et al. (2006) on a typical pyrotechnic retractor. Based on the experimental data of Newberry, a G-force element for the retractor is given as

$$F(t) = F_0 e^{-\sigma_0 (t-t_0)^2} \tag{46}$$

The critical design parameters for the retractor include peak timing $t_0$, pulse width $\sigma_0$ and peak value $F_0$. As a first comparison, 2000N is chosen as base line of peak force value. 3.0s/3.1s/3.2s are selected as different peak timing to investigate the peak timing effect. The maneuver condition is the rollover case. As shown in Figure 17, it can be seen that later peak timing causes a higher possibility of occupant ejection. Peak timing is critical for the design because earlier peak timing can be difficult to determine by sensors assessing whether or not rollover may happen, and later peak timing may not pull the occupant into the crew compartment.

**Figure 17** Comparison for retractor peak timing

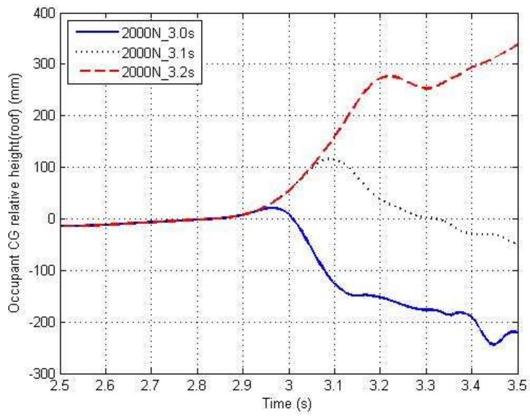


**Figure 18** Comparison for retractor peak force value

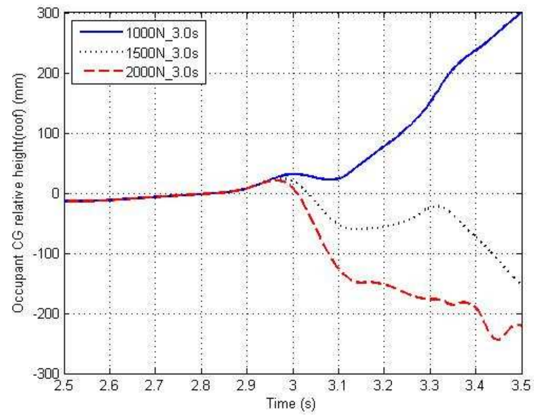


As a second study, 3.0s is chosen as the base line of retractor peak timing, and 1000N/1500N/2000N are selected as different peak force values to investigate the peak force effect. From the results in Figure 18, it is seen that smaller peak force values cause a higher possibility of occupant ejection. The peak force is critical for critical for the design because smaller peak force value could not pull the occupant into the crew compartment, however, a larger peak force value has more possibility to cause injury to the occupant.

It is concluded that peak timing and peak force value as parameters of retractor property are critical for the component design. A representative general force element for the retractor should include these two parameters as design variables.

# 7. Conclusion

Fundamental multidisciplinary structure design technology is proposed for a multibody dynamics systems design problem which may have various options associated with using passive, active, and reactive devices or materials.

The proposed optimization design method can deal with objective functions that are related to dynamic responses of multibody dynamics systems rather than static response, and that satisfy multiple requirements, such as those for designing a vehicle occupant restraint system, under various operating conditions and performance requirements. The proposed advanced topology optimization technique uses an efficient sensitivity analysis technique necessary for practical multidisciplinary multi-constraint problems. A representative model for multidisciplinary components, including possibly passive, active and reactive devices was developed for identifying an optimal layout from a wide open design space.

# Disclaimer

## Acknowledgement

This research was supported by the Automotive Research Center, a US Army Center of Excellence headquartered at the University of Michigan. This support is gratefully acknowledged.

## Reference

[1] Alexe, M. and Sandu, A., (2009), ‘Forward and Adjoint Sensitivity Analysis with Continuous Explicit Runge-Kutta Schemes’, *Applied Mathematics and Computation*, Vol. 208, No. 2, pp. 328-346.

[2] Bendsøe, M. P. and Kikuchi, N., (1988) Generating Optimal Topologies in Structural Design Using a Homogenization Method, *Computer Methods in Applied Mechanics and Engineering*, Vol. 71, No. 2, pp. 197-224.

[3] Bendsøe, M.P., (1989), Optimal Shape Design as a Material Distribution Problem, *Structural and Multidisciplinary Optimization*, Vol. 1, No. 4, pp. 193–202.

[4] Bendsøe, M.P., (1995), *Optimization of Structural Topology, Shape and Material*, Berlin: Springer.

[5] Bendsøe, M.P. and Sigmund, O., (2003), *Topology Optimization: Theory, Method and Applications*, Berlin: Springer.

[6] Berke, L., and Khot, N. S., (1987), Structural Optimization Using Optimality Criteria, In: Mota Soares, C.A. (ed.), The NATO Advanced Study Institute on Computer Aided Optimal Design: Structural and Mechanical Systems on Computer Aided Optimal Design: Structural and Mechanical Systems, (pp. 271–311), Berlin: Springer-Verlag.

[7] Bruls, O., Lemaire, E., Duysinx, P., and Eberhard, P., (2009), Topology Optimization of Structural Components: A Multibody Dynamics-Oriented Approach, *ECCOMAS Thematic Conference*, June 29 – July 2, 2009. Warsaw, Poland.

[8] Cao, Y., Li, S., Petzold, L. and Serban, R., (2003), Adjoint Sensitivity Analysis for Differential Algebraic Equations: The Adjoint DAE System and Its Numerical Solutions, *Journal of Scientific Computation*, Vol. 24, No. 3, pp. 1076-1089.

[9] Chiyo, D., Kodandaramaiah, S. B., Grosh, K., Ma, Z.-D., Raju, B. and Abadi, F. R., (2010), Reactive Structure and Smart Armor for Army’s Future Ground Vehicles, *The 27th Army Science Conference*, November 29 – December 2, 2010, Orlando, FL.

[10] Chung, J., Hulbert, G.M., (1993), A Time Integration Algorithm for Structural Dynamics with Improved Numerical Dissipation: the Generalized-α Method, *Journal of Applied Mechanics*, Vol. 60, No. 2, pp. 371-375.

[11] Dhaher, Y.Y., Tsoumanis, A.D., Houle, T.T., and Rymer, W.Z., (2005), Neuromuscular Reflexes Contribute to Knee Stiffness During Valgus Loading, *Journal of Neurophysiology*, Vol. 93, No. 5, pp. 2698–2709.

[12] Dinant, A. and Kistemaker, B. C., (2007), A Model of Open-loop Control of Equilibrium Position and Stiffness of Human Elbow Joint, *Biological Cybernetics*, Vol. 96, No. 3, pp. 341–350.

[13] Dong, G., Ma, Z.-D., Hulbert, G., Kikuchi, N. and et al. (2009), Function-Oriented Material Design for an Innovative Gunner Restraint System, *The 15th Automotive Research Center Annual Conference*, May 12 - 13, 2009, Ann Arbor, Michigan.
[14] Fleury, C., and Braibant, V., (1986), Structural Optimization: a New Dual Method Using Mixed Variables, *International Journal of Numerical Methods in Engineering*, Vol. 23, No. 3, pp. 409–428.
[15] Fleury, C., (1987), Efficient Approximation Concepts Using Second Order Information, *International Journal of Numerical Methods in Engineering*, Vol. 28, No. 9, pp. 2041–2058.
[16] Granata, K.P., Wilson, S.E., Massimini, A.K. and Gabriel, R., (2004), Active Stiffness of the Ankle in Response to Inertial and Elastic Loads, *Journal of Electromyography and Kinesiology*, Vol 14, No. 5, pp. 599–609.
[17] Gunther, M. and Blickhan, R., (2002), Joint Stiffness of the Ankle and the Knee in Running, *Journal of Biomechanics*, Vol 35, No. 11, pp. 1459–1474.
[18] Hahn, H., (2002), *Rigid Body Dynamics of Mechanisms – 1. Theoretical Basis*, Berlin: Springer.
[19] Hsieh, C.C., Arora, J.S., (1984), Design Sensitivity Analysis and Optimization of Dynamic Response, *Computer Methods in Applied Mechanics and Engineering*, Vol. 43, No. 2, pp. 195-219.
[20] Kang, B.S., Choi, W.S. and Park, G.J., (2001), Structural Optimization Under Equivalent Static Loads Transformed from Dynamic Loads Based on Displacement, *Computers and Structures*, Vol. 79, No. 2, pp. 145 – 154.
[21] Kang, B.S., Park, G.J. and Arora, J.S., (2006), A Review of Optimization of Structures Subjected to Transient Loads, *Structural and Multidisciplinary Optimization*, Vol. 31, No. 2, pp. 81-95.
[22] Leger, A.B. and Milner T.E., (2000), Passive and Active Wrist Joint Stiffness Following Eccentric Exercise, *European Journal of Application Physics*, Vol. 82, No. 5, pp. 472-479.
[23] Livermore Software Technology Corporation (LSTC), (2007), LS-DYNA Keyword User's Manual (Version 971) Appendix N: Rigid Body Dummies, May 2007 Obtained through the Internet http://lstc.com/pdf/ls-dyna_971_manual_k.pdf, [accessed 11/2/2009].
[24] Ma, Z.-D., Kikuchi, N., and Hagiwara, I., (1992), Structural Topology and Shape Optimization for a Frequency Response Problem, *Computational Mechanics*, Vol. 13, No. 3, pp. 157-174.
[25] Ma, Z.-D., Kikuchi, N., (1995a), A New Method of the Sequential Approximate Optimization," *Engineering Optimization*, Vol. 25, pp. 231–253.
[26] Ma, Z.-D., Kikuchi, N., Cheng, H.-C., (1995b), Topological Design for Vibrating Structures, *Computer Methods in Applied Mechanics Engineering*, Vol. 121, No. 1,pp. 259–280.
[27] Ma, Z.-D., Kikuchi, N., Cheng, H.-C., and Hagiwara, I., (1995c), Topological Optimization Technique for Free Vibration Problems, *Journal of Applied Mechanics*, Vol. 62, No. 1, pp. 200–207.

[28] Ma, Z.-D., (2006a), Comparison between Numerical and Experimental Results on Mine Blast Attenuating Seating, Paper *Presented at the 77th Shock & Vibration Symposium*, October 29 -November 2, 2006, Monterey, CA.

[29] Ma, Z.-D., Kikuchi, N., Pierre, C. and Raju, B., (2006b), Multidomain Topology Optimization for Structural and Material Designs, *Journal of Applied Mechanics*, Vol. 73, No. 4, pp. 565-573.

[30] Ma, Z.-D., (2007), Optimization of Fastener System Design for Blast Protection Applications, *Presented at 17th U.S. Army Symposium on Solid Mechanics*, April 2-5, 2007, Baltimore, Maryland.

[31] Ma, Z.-D., Dong, G., Hope, K., and Arepally, S., (2008), Function-Oriented Material Design for an Innovative Gunner Restraint System, *Modeling & Simulation, Testing & Validation (MSTV) Conference '08*, November 18-19, 2008, Warren, MI.

[32] Ma, Z.-D., Dong, G., Hulbert, G.M., Kikuchi, N. and et al., (2010), Fundamental Multidisciplinary Structure Technology with Application to an Innovative Gunner Restraint System for Improved Safety of Military Vehicles, *The 16th Automotive Research Center Annual Conference*, May 10 - 11, 2010, Ann Arbor, Michigan.

[33] Magnusson, S.P., (1988), Passive Properties of Human Skeletal Muscle during Stretch Maneuvers, *Scandinavian Journal of Medicine & Science in Sports*, Vol. 8, No. 2, pp. 65-77.

[34] Newberry, W., Lai, W., Carhart, M., Richards, D., Brown, J. and Raasch, C., (2006), Modeling the Effects of Seat Belt Pretensioners on Occupant Kinematics During Rollover, SAE Technical Paper # 2006-01-0246, *SAE 2006 World Congress, Society of Automotive Engineers*, Warrendale, PA, 2006.

[35] Sigmund, O., (2001), A 99 Line Topology Optimization Code Written in Matlab, *Structural and Multidisciplinary Optimization*, Vol. 21, No. 2, pp. 120–127.

[36] Svanberg, K., (1987), The Method of Moving Asymptotes - A New Method for Structural Optimization, *International Journal of Numerical Methods in Engineering*, Vol. 24, No. 2, pp. 359–373.

[37] Van der Spek, J.H., Veltink, P.H., Hermens, H.J., Koopman, B.F.J.M. and Boom, H.B.K. (2003), A Model-Based Approach to Stabilizing Crutch Supported Paraplegic Standing by Artificial Hip Joint Stiffness, *IEEE Trans Neural System Rehabilitation Engineering*, Vol 11, No. 4, pp. 443-451.

[38] Xu, Y., (1999), A Robust Ensemble Data Method for Identification of Human Joint Mechanical Properties During Movement, *IEEE Transactions on Biomedical Engineering*, Vol. 46, No. 4, pp. 409-419.

[39] Zhou, M. and Rozvany, G.I.N., (1991), The COC Algorithm, Part II: Topological, Geometry and Generalized Shape Optimization, *Computer Methods in Applied Mechanics and Engineering*, Vol. 89, No. 1, pp. 197–224.